THE JOURNAL OF PHYSICAL CHEMISTRY C

pubs.acs.org/JPCC Article

Solution-Mediated Annealing Pathways Are Critical for Supramolecular Ordering of Complex Macrocycles at Surfaces

Henry D. Castillo, Jing Yang, Sibali Debnath, James R. Dobscha, Colleen Q. Trainor, Riley D. Mortensen, Krishnan Raghavachari, Amar H. Flood, Peter J. Ortoleva, and Steven L. Tait*

Cite This: J. Phys. Chem. C 2020, 124, 6689–6699 Read Online

ACCESS | Metrics & More | Article Recommendations | Supporting Information

ABSTRACT: Self-organizations of supramolecular assemblies at surfaces typically achieve highly ordered two-dimensional packing structures due to the negotiation of various intermolecular interactions into a minimum free energy configuration. As we advance these systems toward the long-term goal of achieving programmable surface functionality, however, we consider systems of greater complexity in molecular building-block architecture and in growth conditions. Here, we study the polymorphic self-assembly of tricarbazolo triazolophane macrocycles (tricarb) at the solution/solid interface to determine the underlying pathway that tricarb follows when it transitions between two structures. Tricarb species, depending on peripheral functionalization, self-assemble into kinetically trapped disordered structures or thermodynamically favored ordered honeycomb structures. Experiments varying pre- and post-deposition conditions (solubility, concentration, and temperature) suggest that a solution-mediated annealing pathway, as opposed to an on-surface rearrangement, is key to a transition from disordered structures to honeycomb. Molecular dynamic simulations provide nanoscale insights into the roles of peripheral groups and solvent molecules in self-assembly. Substituents on the exterior of the molecule not only affect solubility but also stabilize tricarb−tricarb hydrogen-bonded structures. Peripheral groups influence the formation/re-formation and strength of adsorbate−adsorbate contacts and also limit solvent interactions about a macrocyclic core. The combination of simulation and experiment demonstrates the role of the solution-mediated annealing pathway in the self-assembly of complex supramolecular systems.

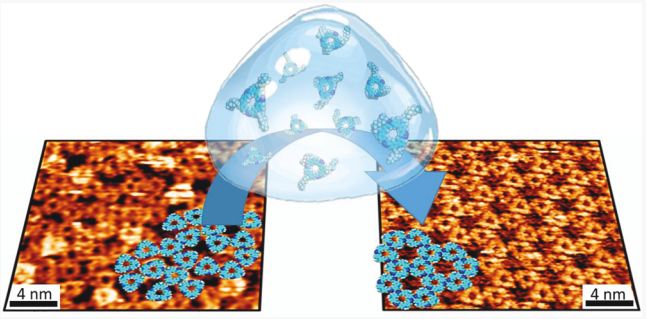

INTRODUCTION

Since the pioneering work by Rabe,[1] studies of molecular self-assembly at the solution/solid interface have produced great strides in understanding how supramolecular interactions affect the structure of self-assemblies and have also produced functional and potentially useful materials.[2] One avenue of interest is in developing polymorphic systems in which one or a few molecular building blocks can be programmed to self-assemble into several distinct structures, each of which has unique properties and functions. Control over the stability of each structure and transitions between structures in a polymorphic system can be obtained through peripheral functionalization in the molecular design or by controlling assembly conditions, such as concentration, temperature, solvent, or host−guest complexation.[3−11]

Understanding the underlying mechanisms by which supramolecular systems transition between polymorphs is essential in improving control and understanding of self-assembly. To this end, it is well-known that solvation directs polymorphic self-assembly,[10−17] and several studies have quantified the kinetics and thermodynamics related to solvation on self-assembly.[18−22] In polymer thin films, solvent annealing has been extensively employed to alter packing and also to alter macroscopic properties and device performance.[23−32] However, examination of solution-mediated annealing pathways has not been conducted for 2D self-assembly at the solution/solid interface. Here, we investigate the role of solvation and solvent annealing in directing the disordered/ordered self-assembly of a polymorphic system of macrocycles at the solution/graphite interface. We do this using a series of macrocycle molecules (Scheme 1) that are examined by high-resolution scanning tunneling microscopy (STM) and molecular dynamics simulations (MD).

Disordered structures have been given little attention at the solution/solid interface.[33,34] With few exceptions,[35−40] the majority of systems studied to date have concentrated on neatly ordered structures and transitions between them. For

Received: December 23, 2019
Revised: February 22, 2020
Published: March 2, 2020

https://dx.doi.org/10.1021/acs.jpcc.9b11867
J. Phys. Chem. C 2020, 124, 6689−6699

Scheme 1. Tricarbazolo Triazolophane Macrocycles (Tricarb) with Various Peripheral Groups

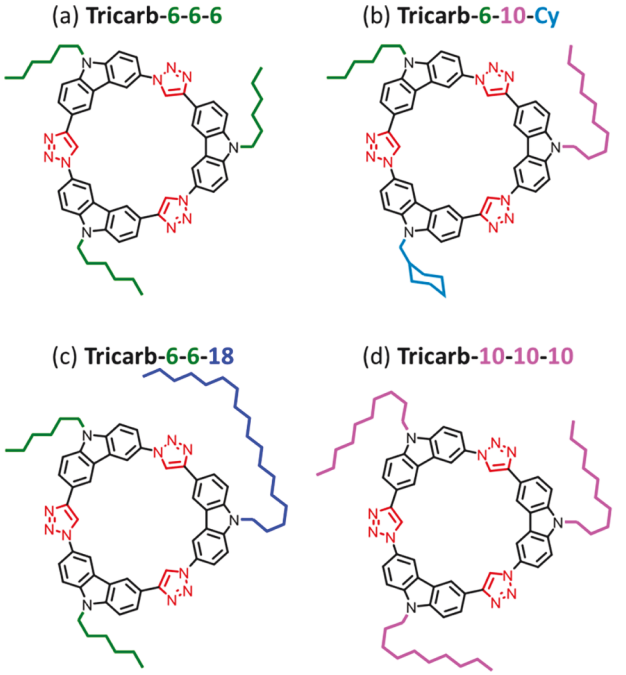

macromolecular systems (e.g., proteins or polymers) and thin films, disordered packing and disorder/order transitions are essential for proper function.[41−49] In proteins, proper function depends on transitions between ordered/disordered structures and interactions between ordered/disordered domains.[41−44] In organic thin films, order/disorder transitions are observed with increasing dopant concentration.[49] In a diblock copolymer system, an order/disorder transition has been controlled by temperature, which shifts the hydrophilicity of the molecular units.[48] Just as in macromolecular systems and thin films where understanding disorder is essential for understanding function, understanding disordered self-assembly is an important facet in producing more complex self-assembled structures.

The majority of previous studies of molecular assembly at surfaces have been limited by the temporal resolution of scanning probe techniques. To a lesser extent, molecular simulations have been used to gain novel molecular-level insights into solvent−adsorbate−surface interactions and processes that are not observable with experiment alone. Expanding our understanding of nanoscale supramolecular interactions and processes is essential in developing a deeper understanding of self-assembly.[33,50−58]

Previous work showed that tricarbazolo triazolophane macrocycles (tricarb) functionalized with decyl chains (tricarb-10-10-10, Scheme 1d) self-assemble into an ordered honeycomb packing at the solution/solid interface.[59] High-resolution STM imaging of these systems allows for precise determination of the relative molecular orientation and spacing, which leads to models of the supramolecular packing that indicate stabilizing hydrogen-bonding interactions.[59] STM findings were supported by a subsequent crystal structure in a recent work.[60] It was also observed in the STM experiments that the peripheral alkyl chains tend to be excluded from surface adsorption; that is, the chains back-fold into solution and do not directly impact structure. However, two recent experimental and computational studies using different peripheral alkyl chains of tricarb[9,56] reveal that chain length and functionalization symmetry can play a major role in tricarb self-assembly structure. We were therefore interested to examine the role of the chain length; this led to discovery of a disordered packing phase on the surface,[9] and here we report that the conversion of that disordered structure to an ordered structure demonstrates a solution-mediated annealing pathway.

In this work, we examine the role of solvation and temperature in influencing whether various tricarb species (Scheme 1) access the ordered honeycomb or disordered structure, and we demonstrate that a solution-mediated pathway through solvent annealing is essential to transition disordered structures to ordered honeycomb. STM experiments are complemented by atom-resolved MD simulations to examine nanoscale dynamics of several tricarb macrocycles and solvents on graphite.

METHODS

All tricarb macrocycles were prepared following previously published procedures: tricarb-6-6-6,[60] tricarb-10-10-10,[59] tricarb-6-6-18,[9] and tricarb-6-10-Cy.[9]

Experimental STM Procedures. STM experiments were performed on an Agilent Technologies 5500 PicoPlus STM using a Picoscan 1.18.1 controller in constant-current mode. Tips were mechanically cut from Pt/Ir wire (80:20, 0.25 mm diameter, nanoScience Instruments). Voltage pulses between 2 and 10 V with 1−3 ms duration were occasionally conducted to improve image quality. Unless noted, all experiments were conducted at room temperature.

Samples were prepared by dropping 6 μL of solution via micropipet onto a freshly cleaved highly ordered pyrolytic graphite (HOPG) surface (ZYB, 10 mm × 10 mm × 1 mm, NanoAndMore U.S.A.) at room temperature, unless otherwise specified. In some experiments the HOPG surface was heated or cooled before deposition, as noted below. HOPG was mechanically cleaved by using Scotch tape, and a minor circular impression was made in the HOPG surface by pressing a Viton O-ring on the surface for several seconds. The impression prevented the liquid sample from wicking off the HOPG surface. Solutions were prepared with 1,2,4-trichlorobenzene (≥99%), octanoic acid (≥99%), and toluene (≥99.5%). Typical scanning parameters ranged from I_t = 0.05 to 1.7 nA and V_{sample} = −0.4 to −1.2 V (Table S1).

The STM sample stage has an integrated heater that allows for temperature control during deposition and scanning. Low-temperature STM was accomplished by placing a container of dry ice below the sample plate during scanning. In both cases, the temperature was monitored using a thermocouple that is directly attached to the sample stage. Samples heated to 100 °C were subsequently cooled to 30 °C at a rate of −1 °C/min. As solvent evaporated, warm solvent was added to keep solution volume and concentration approximately constant. The amount of solvent added was estimated by visual inspection of the solution droplet size.

Molecular Dynamics Simulation Design and Conditions. Each system in Table S4 consisted of a four-layer AB-stacked graphene (HOPG), preformed honeycomb structure of tricarb molecules, and explicit solvent molecules (if not in a vacuum). The honeycomb structures were constructed with the guidance of STM images (Figure S3), following the strategy introduced in the Supporting Information in a recent report.[56] The preformed honeycomb structure of tricarb macrocycles was placed 3.5 Å above the HOPG with all

https://dx.doi.org/10.1021/acs.jpcc.9b11867
J. Phys. Chem. C 2020, 124, 6689−6699

alkyl tails desorbed from the HOPG. See the Supporting Information of our recent report for a detailed description of the initial configuration design.

MD simulations were performed using the molecular modeling software package GROMACS 5.0.4 with customized force fields (Section S3 of the Supporting Information).[61,62] The visual molecular dynamics (VMD) molecular graphics software version 1.9.3 was used for visualization purposes.[63] For each simulation, energy minimization was performed first via steepest descent algorithm, followed with the conjugate gradient algorithm. Then, the system was thermalized via 40 ps NVT simulation at 300 K using V-rescale thermostat.[64] The pressure was maintained at 1 bar with the Berendsen pressure coupling. The position restraint algorithm was used when solvents molecules were present; this allowed solvent molecules to properly relax around tricarb macrocycles as well as on the HOPG.

The product runs were performed under NVT conditions by using a Nosé−Hoover thermostat at 300 K with a coupling constant of 0.5 ps. The vdW interaction was modeled via Lennard-Jones potential with a switch scheme. The Lennard-Jones potential was normal out to 1.5 nm, after which it was switched off to reach zero at 1.7 nm. The Coulomb interactions were calculated by using the reaction-field-zero method[65] with a 1.7 nm cutoff radius. Periodic boundary conditions based on cubic computational boxes were used for system with solvent. Considering the thickness of solvent layer was twice the distance of the non-bonded interaction range and tricarb macrocycles were never observed to desorb from the HOPG, it is guaranteed that tricarb molecules do not interact with any virtual images.

RESULTS AND DISCUSSION

Honeycomb and Disordered Structures. We discovered structurally disordered domains in the self-assembly of three tricarb species (Scheme 1a−c) above some concentration threshold (Figure 1b). The disordered phase is only observed for three of seven variations of tricarb that we have tested (Figure S21). These disordered structures are in sharp contrast to our previous report of the assembly of tricarb-10-10-10. This C_3 symmetric molecule, substituted with three peripheral decyl chains, exhibited highly ordered self-assembly on HOPG, forming a honeycomb packing at higher concentrations and a "flower" phase packing at lower concentrations.[59] That honeycomb structure is also observed for the new tricarb species, but now in coexistence with the disordered structure at intermediate concentrations. The disordered structure has no long-range order and contains a variety of local tricarb−tricarb contacts,[56] although there are two frequently observed hydrogen bonding motifs (Figures 1e,f). Randomly tiled terphenyltetracarboxylic acid structures are similar in their variety of molecule−molecule contacts.[38]

The 2D packing density of molecules within the disordered domains ($\sigma_{disordered}$ = 0.34 molecules/nm^2) is slightly higher than for honeycomb ($\sigma_{honeycomb}$ = 0.28 molecules/nm^2). As the deposition concentration is further increased, the disordered domains cover more of the surface (Figure 1c); thus, the total tricarb surface coverage increases.

The concentration boundary between the formation of ordered vs disordered structures depends on the length of the peripheral alkyl chain (Figure 2). Tricarb with three $-C_{10}H_{21}$ units, tricarb-10-10-10 (Scheme 1d), never self-assembles into disordered packing, even at concentrations up to the point at which it precipitates from solution (3 mM, Figure S6). However, with shorter $-C_6H_{13}$ peripheral groups, tricarb-6-6-6 (Scheme 1a) exhibits some disordered domains as low as ∼3 μM, and the surface is completely covered by disordered domains at deposition concentrations of 100 μM (Figure S7). Note that for tricarb-6-6-6 a 100 μM solution in TCB precipitates after several hours, but a 1 mM tricarb-10-10-10 solution in TCB is stable for several days.

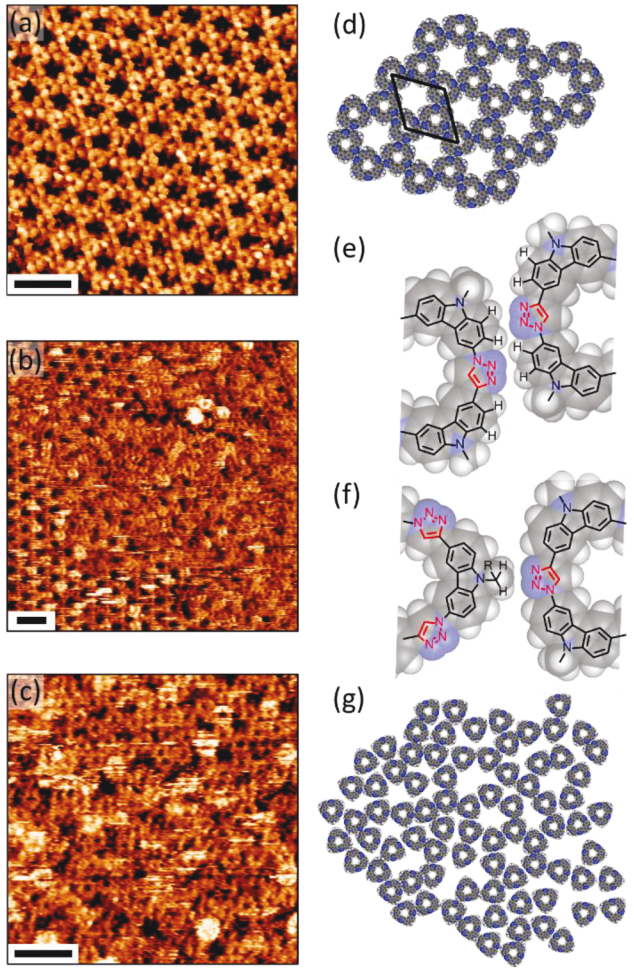

Figure 1. STM images of tricarb-6-10-Cy (Cy = methylcyclohexane) in TCB (6 μL solution) on HOPG at 20 °C. (a) Deposition at 10 μM results in exclusively honeycomb, (b) coexistence of disordered and honeycomb structures at 300 μM, and (c) disordered structure at 300 μM. At 1 mM, exclusively disordered structures are formed. Supramolecular packing models of (d) honeycomb and (g) disordered with detailed examples of (e) triazole−carbazole and (f) methylene−triazole non-traditional hydrogen bonding. The unit cell in (d) has dimensions of $a = b = 2.94 \pm 0.08$ nm and $\gamma = 59 \pm 3°$. Scale bars: 5 nm.

The lower symmetry tricarb-6-6-18 (Scheme 1c) has the same mass as tricarb-10-10-10 but has nonsymmetric AAB peripheral groups with two $-C_6H_{13}$ chains and one $-C_{18}H_{37}$ chain. In this case, some disordered structures are observed with tricarb-6-6-18 deposited at a concentration of ∼200 μM. Note that tricarb-6-6-18 also forms a unique gap structure at low concentrations that is not observed in other tricarb species. At 200 μM, all three structures (honeycomb, gap, and disordered) coexist, but honeycomb is dominant.[9] Complete surface coverage of disordered structures is observed at a

https://dx.doi.org/10.1021/acs.jpcc.9b11867
J. Phys. Chem. C 2020, 124, 6689−6699

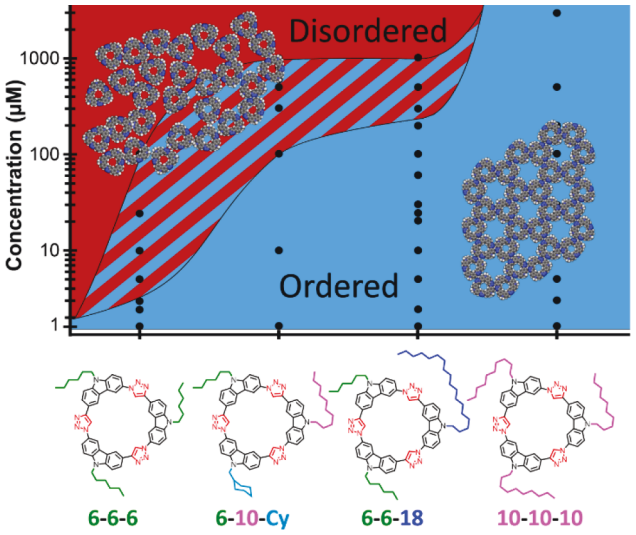

Figure 2. Tricarb self-assembly structure as a function of concentration and peripheral functionalization (solvent: TCB; temperature: 20 °C). Striped area represents concentrations where disordered and ordered structures coexist. Dots represent tested concentrations. Disordered structure is a kinetically trapped state, as discussed in the text.

concentration of 1 mM (Figure 2). The deposition concentrations required to achieve disordered structures for tricarb-6-6-18 are significantly higher than for tricarb-6-6-6.

With an ABC pattern of $-C_6H_{13}$, $-C_{10}H_{21}$, and methylcyclohexyl groups (Scheme 1b), tricarb-6-10-Cy self-assembles into honeycomb and disordered packing structures that under some conditions are observed to coexist (Figure 1a–c). The concentration regime in which tricarb-6-10-Cy self-assembles into honeycomb or disordered structure is similar to that of tricarb-6-6-18 (Figure 2).

Influence of Deposition Temperature. We conducted experiments at different deposition temperatures to explore the relative stability of the disordered and honeycomb structures (Table 1). When a room temperature solution of either tricarb-6-10-Cy or tricarb-6-6-18 is deposited on an HOPG surface (300 μM was chosen for a 1:1 honeycomb:disorder population at room temperature in TCB), the crystalline honeycomb structure is favored at higher temperature and the disordered structure is favored at lower temperature (Figure 3 and Figure S8; Table 1).

Table 1. Fractional Honeycomb Surface Coverage, θ_{HC}, in Self-Assembly of Tricarb as Deposition Temperature and Solvent Are Varied[a]

tricarb-6-10-Cy (300 μM) and tricarb-6-6-18 (300 μM)			
T_{dep} (°C)	8	20	50
θ_{HC}	0.2	0.5	0.8
tricarb-6-10-Cy (300 μM)			
solvent	OA/TCB	TCB	toluene/TCB
θ_{HC}	<0.1	≈ 0.5	>0.8
tricarb-6-6-18 (250 μM)			
solvent	OA/TCB	TCB	toluene/TCB
θ_{HC}	0	≈ 0.5	>0.7

[a] θ_{HC} = fractional honeycomb coverage; T_{dep} = deposition temperature.

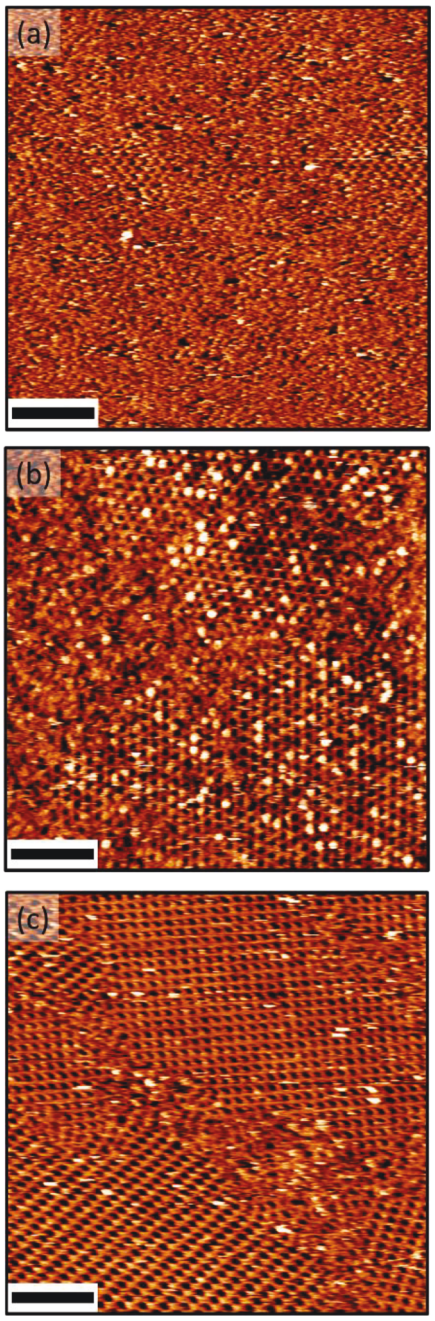

Figure 3. Three different samples of tricarb-6-10-Cy (300 μM, solvent: TCB) deposited at surface temperatures of (a) 8, (b) 20, and (c) 50 °C. More honeycomb domains are present when deposited at 50 °C (c), and more disordered domains are present when deposited at 8 °C (a). Scale bars = 20 nm.

In an equilibrium picture, if one considers only the configurational entropy of the 2D arrangement of tricarb molecules on the surface, then the disordered structure clearly has an entropic advantage. The observation that honeycomb is favored at higher temperature indicates that the role of the solvent and dissolved tricarb state are also important considerations in the growth behavior; i.e., a naïve 2D model of tricarb configurational entropy is inadequate to describe the system as this would contradict the expectation of entropy stabilization at high temperature.[66] The high-temperature stability of the ordered honeycomb structure also suggests that although the disordered structure is kinetically accessible

https://dx.doi.org/10.1021/acs.jpcc.9b11867
J. Phys. Chem. C 2020, 124, 6689–6699

under certain conditions, the honeycomb state is thermodynamically favored.

Postdeposition Treatment. Remarkably, although the packing structure depends strongly on deposition temperature, we did not see a change in either the disordered structure or the honeycomb structure with postdeposition heating or cooling (Figure S9); that is, the structure determined by the deposition temperature is stable in either case. For example, tricarb-6-10-Cy (300 μM) deposited at 50 °C is mostly composed of honeycomb. Cooling this sample down to 20 and 8 °C did not change the ratio of honeycomb to disordered on the surface even after 24 h. However, the same molecule at higher concentration (1000 μM) deposited at 20 °C only forms disordered structure. When that sample is heated at 100 °C for 10 min and subsequently cooled to 30 °C, it remains as only disordered structure, even after 10 h.

This strong history dependence clearly points to a kinetic trapping effect as we do not see the system equilibrate to a specific packing arrangement at a given temperature. Similar observations of thermal-history-dependent self-assemblies have been observed at the solution/solid interface with alkyl-functionalized tristyrylbenzene[37] and dehydrobenzoannulene.[11] For both systems, the porous and less dense structure was thermodynamically favored and formed when deposition occurred at higher temperatures, but at lower deposition temperatures, the kinetically favored and denser packing structure formed.[11,37]

The lack of ordering with post-deposition annealing may indicate that on-surface rearrangement is not an important pathway to lead to the ordered honeycomb structure. This interpretation is supported by the observation in our studies that the larger molecules, which should have a lower on-surface mobility, are more likely to form the honeycomb structure.

We also found that *in situ* modification of concentration does not induce post-assembly structural changes. In TCB at 20 °C, tricarb-6-10-Cy self-assembles exclusively into honeycomb at 10 μM. Upon *in situ* addition of a 1 mM solution (final tricarb-6-10-Cy concentration: 800 μM), the surface structure remains exclusively honeycomb, even after 12 h. When a 1 mM solution of tricarb-6-10-Cy is directly deposited onto clean HOPG at 20 °C, tricarb-6-10-Cy instead self-assembles exclusively into the disordered structure. After *in situ* addition of neat TCB to that sample to achieve a final concentration of 100 μM, only disordered structures were observed. Remarkably, even after 12 h and heating to 50 °C, only the disordered structure is observed. A 100 μM solution of tricarb-6-10-Cy directly deposited onto clean HOPG instead self-assembles into mostly honeycomb (over 90% surface coverage).

Post-deposition experiments indicate that a large energy barrier between honeycomb and disordered assembly stems from the significant stabilizing influence of tricarb−tricarb and tricarb−surface interactions. This observation is different from other self-assembled systems at the solution/HOPG interface in which post-self-assembly modification was more easily facilitated.[5,11,67−70]

Effect of Solubility. Changing the solubility of tricarb alters self-assembly to either favor honeycomb by improving solubility or favor disordered structures by decreasing solubility. The solubility of tricarb molecules was changed by altering the solvent composition of the solution (Figure 4 and Figure S10; Table 1) or by altering the peripheral groups of tricarb (Figure 2).

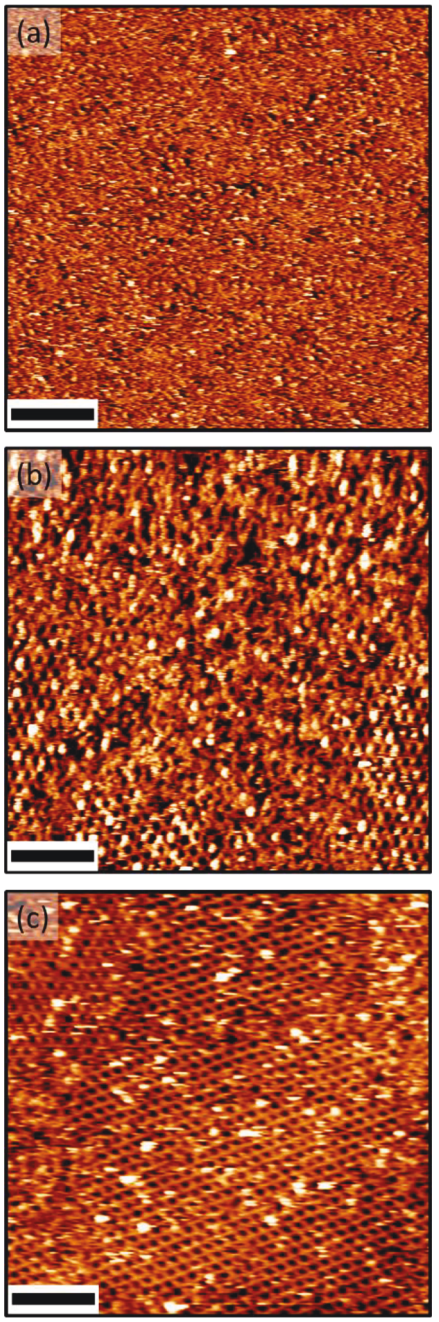

Figure 4. Three different samples of tricarb-6-10-Cy (300 μM) with different solvent compositions. (a) Solvent composed of 1:1 (by volume) of TCB and octanoic acid (OA). Only disordered structure is observed. (b) Solvent composed of only TCB. Both disordered and honeycomb structures are present. (c) Solvent composed of 1:1 (by volume) of TCB and toluene. Almost entire surface is covered with honeycomb. Note that toluene is volatile and evaporates within tens of seconds after deposition. The concentration of this sample while scanning is 600 μM. Scale bars = 20 nm.

Changing solvent composition is a well-established method to alter the solution phase kinetics and structure of protein assemblies[43] and of macrocycles,[71,72] including tricarb.[59] At the solution/solid interface, as solubility decreases, trimesic acid self-assembles into a more dense packing,[13] ferrocene derivatives self-assemble into kinetically trapped islands,[16] and annulene derivatives self-assemble into more dense and kinetically trapped structures.[17] In our study, solvent mixtures

https://dx.doi.org/10.1021/acs.jpcc.9b11867
J. Phys. Chem. C 2020, 124, 6689−6699

were used to shift the relative stability of tricarb in the adsorbed state vs solvated state: TCB was mixed with toluene (1:1 by volume) to increase tricarb solubility or with octanoic acid (OA; 1:1 by volume) to reduce solubility.

When deposited from TCB/OA solvent, tricarb-6-10-Cy (300 μM) self-assembles into almost all disordered structures (<10% honeycomb) and tricarb-6-6-18 (250 μM) self-assembles into only disordered structure. Those same two molecules at the same concentrations in TCB form honeycomb and disordered structures in roughly equal amounts (each 50 ± 10%). As the solubility is further increased by the addition of toluene to create a TCB/toluene mixture, the tricarb-6-10-Cy macrocycle (300 μM) self-assembles into over 80% honeycomb while tricarb-6-6-18 (250 μM) self-assembles into 70 ± 10% honeycomb. It is important to note that toluene is volatile; thus, the solvent mixture is only a transient effect. By lengthening the duration of the solvent mixture, either by adding more toluene or impeding toluene evaporation by placing the sample in a closed container, more honeycomb is formed. We also note that due to the toluene evaporation, the concentration of tricarb doubles during the experiment; if an experiment is started with that high concentration, we only observe disordered structure.

As solvent composition of the molecule affects surface packing, we also adjusted the solubility by molecular design, that is, by modification of the peripheral functional groups that largely determine solubility. Of the seven tricarb species tested (Figure 2 and Figure S21), only tricarb-6-6-6, tricarb-6-10-Cy, and tricarb-6-6-18 self-assemble into a disordered structure. These three species have shorter peripheral groups (hexyl and methylcyclohexyl moieties) and display the lowest solubility of the other tricarb variations. Counterintuitively, the tricarb species with the lowest (individual) conformational entropy (shortest alkyl chains, tricarb-6-6-6) self-assembles in the disordered structure; i.e., it has the greatest tendency to form the packing structure with the highest packing entropy. Conversely, the tricarb species with the highest solubility in TCB (longest alkyl chains; tricarb-8-8-8, tricarb-9-9-9, tricarb-10-10-10, and tricarb-18-18-18; Figure S21) do not self-assemble in the disordered structure but only form the ordered honeycomb structure, which has lower packing entropy. As discussed above, focusing only on the 2D configurational entropy of adsorbed tricarb does not provide a complete picture as there are other compensating entropic effects in this system.

Honeycomb Domain Size. Increased solubility and increased deposition temperature not only promote honeycomb structure over disordered structure self-assembly, but also promote the assembly of larger honeycomb domains. We have analyzed the domain sizes for the honeycomb structure for multiple tricarb species, solvents, concentrations, and deposition temperatures (Table S6). Higher concentrations result in smaller domains of ordered structures, as expected for a kinetically limited growth mechanism. For example, at 100 μM, tricarb-10-10-10 forms honeycomb domains in the range of ~600 to >10000 nm^2, but at 3000 μM the domain size is only 30−6500 nm^2. Comparison is limited to this concentration range in which the honeycomb structure is observed and tricarb is readily soluble.

Of the four tricarb species studied in this work, only two, tricarb-6-6-6 and tricarb-6-10-Cy, have an overlapping concentration range in which honeycomb is the exclusive packing structure. Thus, these allow for a direct comparison of the impact of macrocycle structure on domain size at the same concentration. At the overlapping concentration (1 μM), there is no difference in honeycomb domain size between these molecules (Table S6).

Domain size, like ordered vs disordered packing, is also strongly impacted by solvent choice or by deposition temperature. Either tricarb-6-6-18 or tricarb-6-10-Cy (each at 300 μM) produces mostly disordered structure with small honeycomb domain areas of ~500 nm^2 or less when deposited either from TCB/OA or at 8 °C. However, deposition of the same tricarb species from TCB/toluene or at 50 °C (both of which promote honeycomb self-assembly) results in larger honeycomb domains of ~1500 to 8000 nm^2.

These observations together show that the same conditions that promote ordered self-assembly (e.g., lower concentrations, better solubility, or higher temperatures) also result in larger honeycomb domains, while conditions that promote disordered self-assembly (e.g., higher concentrations, lower solubility, or lower temperatures) result in smaller honeycomb domains.

Solvent Annealing. Unlike thermal annealing, which cannot induce a post-self-assembly modification, *in situ* addition of toluene promotes the transition to honeycomb from disordered structures through solvent annealing. At the lowest concentration (1 mM, 1 μL, TCB solvent) at which tricarb-6-10-Cy exclusively forms the disordered structure, the *in situ* addition of 16 μL of toluene can induce a post-assembly change to ~70% honeycomb surface coverage (Figure S11a). This structural change is observed immediately in STM imaging. The honeycomb structures are stable over the course of several hours. The same experiment with TCB has no effect; with *in situ* addition of 16 μL of TCB to a tricarb-6-10-Cy sample (1 mM, 1 μL, TCB solvent), no change in self-assembly was achieved even after 4 h. During the course of ~5 min, the added toluene rapidly evaporates with the droplet size shrinking back to original size. This observation suggests that the structure change is not a transition between different thermodynamically favored structures but an annealing effect to overcome a kinetic barrier.

Toluene annealing has a lessened effect with tricarb-6-6-18. At the lowest concentration (1 mM, 1 μL, TCB solvent) at which tricarb-6-6-18 forms exclusively disordered structures, no change in self-assembly occurs after *in situ* addition of 16 μL of toluene. However, at a lower concentration at which tricarb-6-6-18 forms ~10% honeycomb (500 μM, 1 μL, TCB solvent), *in situ* addition of 16 μL of toluene changes the surface coverage to roughly 30% honeycomb.

Although deposition from octanoic acid (OA) promotes the disordered structure, *in situ* addition of OA (2 μL) into a tricarb-6-10-Cy sample (10 μM, 2 μL, TCB solvent) that is exclusively honeycomb does not produce any change in structure (Figure S11b). In other words, while *in situ* toluene solvent addition can induce a post-self-assembly transition from disordered structure to honeycomb structure, we have not observed the reverse process, in which a different solvent addition would facilitate a change from honeycomb to the disordered structure. This along with variable temperature studies (*vide supra*) indicates that honeycomb is the thermodynamically favored structure.

Several prior studies have also reported improvement in molecular structures due to solvent effects.[16,23−28,31,32] Analogous solvent annealing results have been widely reported in polymer systems as a viable pathway to improve order and

https://dx.doi.org/10.1021/acs.jpcc.9b11867
J. Phys. Chem. C 2020, 124, 6689−6699

function.[23−32] Solvent annealing can form more ordered structures both at larger length scales and at faster time scales compared to thermal annealing[24,25] and has other advantages over thermal annealing, including that degradation of the monomers is not an issue[23,25,26] and that solvent evaporation can be better controlled.[24]

In light of these prior studies, our observations of (1) solubility-dependent ordering upon deposition, (2) temperature-dependent ordering, (3) honeycomb domain size, and (4) structural ordering with solvent addition suggest a solvent-annealing pathway. Together, these results show that the increased solubility of tricarb allows a new assembly mechanism toward ordered honeycomb structure. We suggest that this mechanism consists of some tricarb desorption from the surface into a solvated state, allowing other tricarb to reassemble into the lower density honeycomb packing. This proposed solvent-mediated annealing mechanism, involving desorption and readsorption steps, is consistent with the ineffectiveness of thermal annealing to produce a transition and with our observation that larger (more soluble and less mobile) tricarb species more readily form honeycomb structures. Our experimental observations are not consistent with a purely on-surface rearrangement mechanism.

Adsorbate−Adsorbate and Adsorbate−Substrate Interactions. MD simulations provide further validation that honeycomb is thermodynamically favored. At the vacuum/HOPG interface, simulations of tricarb-1-1-1 showed that it formed two packing structures: ordered honeycomb packing and a high density packing with only methyl−triazole intermolecular contacts (Figure 1f). We calculated the average energy needed to remove one tricarb-1-1-1 molecule from an array of 52 molecules: 538 ± 6 kJ/mol for the honeycomb structure and 500 ± 8 kJ/mol for the high-density packing structure (Figure S12). The honeycomb structure is enthalpically favorable.

Disordered structures have a higher packing density ($\sigma_{disordered}$ = 0.34 molecules/nm^2) than honeycomb structures ($\sigma_{honeycomb}$ = 0.28 molecules/nm^2), but the regular triazole−carbazole hydrogen bonding between tricarb molecules in honeycomb apparently outweighs any energetic advantage due to the higher packing density in the disordered structure. Triazole−carbazole contacts, which are present in both honeycomb and disordered structures, are 12 kJ/mol more favorable than triazole−methyl interactions, which are only observed in the disordered structures (Figure S13). Other studies have shown examples of low-density supramolecular assemblies stabilized by advantageous intermolecular interactions.[73−77]

Alkyl Chains Protect Honeycomb Stability. Comparison of tricarb simulations of different peripheral alkyl length suggests that triazole−carbazole hydrogen bonding alone fails to preserve the experimentally observed honeycomb structure. For simulations with explicit TCB solvent, tricarb-1-1-1 (82.3 mM) deteriorates into disordered structure, tricarb-6-6-6 (67 mM) lost honeycomb structure on the edges, and tricarb-10-10-10 (61.2 mM) remains in the stable honeycomb structure (Figure S4), in spite of the fact that the triazole−carbazole contacts for these are identical. These observations are consistent with our previous MD work simulating tricarb at the vacuum/HOPG interface, where interactions between peripheral groups and the macrocyclic core promote ordered packing.[56] These MD observations are made on a simulation time scale of up to 100 ns. We note that the computational cost of these atomistic simulations does not currently allow for the significantly longer time scales that would be required to simulate surface self-assembly starting from solution or structural transformations between surface structures.

MD simulations allow molecular-level observation of the loss of order in tricarb-1-1-1 (and partially in tricarb-6-6-6) honeycomb structure, and this loss is triggered by the insertion of TCB solvent molecules. Adsorbed tricarb molecules are surrounded by TCB molecules, both co-adsorbed on HOPG and in solution, that can attack the tricarb−tricarb interaction. TCB molecules can insert themselves in between tricarb molecules, form local dipole−dipole interactions with the sides of the tricarb macrocycle, and lay flat on the surface to fully disrupt the tricarb−tricarb hydrogen bonding (Figure 5 and Figure S15).

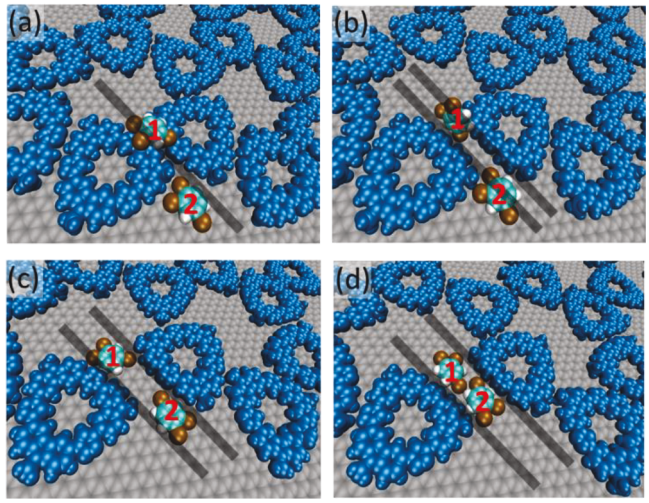

Figure 5. Representative example of loss of honeycomb structure triggered by the insertion of TCB molecules. Two TCB molecules (one from solution and one adsorbed on HOPG) make a concerted insertion in between tricarb macrocycles. Tricarb-1-1-1 macrocycles are in blue. TCB molecules are colored by atom type (Cl = ochre, H = white, C = cyan). (a) Initially, TCB1 hovers in solution above two contacting macrocycles, while TCB2 is initially adsorbed to the HOPG. (b) After 25 ps, TCB1 moves in between two macrocycles and (c) then lays down on the HOPG. (c) After 0.5 ns, TCB2 migrates in between the two macrocycles. (d) After 25 ps, both TCB molecules reorient themselves to form hydrogen-bonding contacts between each other and tricarb macrocycles.

When the solvent is changed to toluene in MD simulations, there is much less deterioration of the honeycomb structure. Tricarb-1-1-1 (82.3 mM) deteriorates into the disordered structure at a slower rate in toluene (Figure S20) compared to TCB (Figure S19). Both tricarb-6-6-6 (67 mM) and tricarb-10-10-10 (61.2 mM) preserve the honeycomb structure (Figure S5) in toluene.

The large-scale difference between the two solvents can be rationalized by local observations from MD. When TCB molecules adsorb between two tricarbs on the surface, they have a mean residence time of 100 ps to 10 ns, while toluene has a typical residence time of only tens of picoseconds. Therefore, although fractures between neighboring tricarbs (for tricarb-10-10-10 and tricarb-6-6-6) are more frequently observed in toluene than in TCB, these fractures are more frequently seen to heal themselves in toluene (Figure S18). Even fractures between tricarb-1-1-1 molecules are able to heal

https://dx.doi.org/10.1021/acs.jpcc.9b11867
J. Phys. Chem. C 2020, 124, 6689−6699

themselves in toluene (Figure S17). In TCB, self-healing is only observed with tricarb-10-10-10 (Figure S14), while disruptions in the honeycomb lattice of tricarb-6-6-6 and tricarb-1-1-1 are not reversible. We also note that deterioration of honeycomb networks in toluene only starts from domain edges (Figure S20), but in TCB, solvent disruption occurs throughout the honeycomb domain (Figure S19).

The strong dependence of these effects on peripheral alkyl chain length points to important roles of the peripheral groups on honeycomb stability. First, the honeycomb pores are filled with tricarb alkyl chains and with co-adsorbed solvent. Longer alkyl chains sterically block the area around the tricarb−tricarb contacts that the solvent would need to access to disrupt the structure (Figure 6 and Figure S16). Comparing simulations of

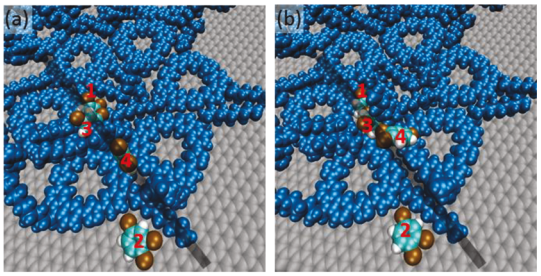

Figure 6. Representative example of peripheral alkyl chains preventing solvent (TCB) insertion in between tricarb. Tricarb-10-10-10 macrocycles are in blue. TCB molecules are colored by atom type (Cl = ochre, H = white, C = cyan). (a) Initially, TCB1 and TCB2 are adsorbed onto HOPG near macrocycles, while TCB3 and TCB4 are partially adsorbed. (b) After 75 ps, none of the TCBs can migrate in between macrocycles, and TCB4 migrates away. Noticeably, an adsorbed alkyl chain blocks TCB2 from further contact with the tricarb cores.

tricarb-10-10-10, tricarb-6-6-6, and tricarb-1-1-1 (Figures S4 and S5), we see that larger side chains allow less coadsorbed solvent within the honeycomb pores. Second, alkyl chains that are not adsorbed to the surface tend to stay in the vicinity of the tricarb macrocycle sides (Figure 6, Figures S4 and S5) and thus provide a steric block against direct attack of solvent molecules to the hydrogen-bonding tricarb−tricarb contact.

CONCLUSIONS

These experiments demonstrate that the transition from tricarb disordered structure to the thermodynamically favored honeycomb structure involves a solution-mediated pathway. The ordered honeycomb structure is favored in initial growth by high deposition temperature, better solvent, or longer peripheral chains; each of those increases solubility of the tricarb and thus facilitates a solvent annealing pathway. Thermal annealing, however, is ineffective to induce postdeposition structural change from the disordered structure to the honeycomb structure, which suggests that an on-surface rearrangement pathway is not accessible. A solution-mediated pathway, facilitated by toluene addition (but not by trichlorobenzene or octanoic acid), does allow *in situ* structural rearrangement from disordered structure to honeycomb. MD simulations corroborate that the honeycomb structure, although it has a lower packing density, is energetically favored relative to the disordered structure due to more favorable lateral hydrogen-bonding contacts.

Experiments show that the larger, more soluble tricarb species access the honeycomb structure over a wider concentration range than smaller species. MD simulations support the higher stability of larger tricarb species in honeycomb domains through molecular-level insight. The simulations demonstrate that longer peripheral groups impede the disruption of adsorbed tricarb−tricarb contacts by blocking solvent insertion. The alkyl chains also preserve tricarb honeycomb order by increasing adsorbate−adsorbate and adsorbate−substrate vdW interactions. This combined STM and MD investigation demonstrates that macrocycle−macrocycle contacts are interrupted by solvent, that these contacts can self-heal, that longer peripheral chains stabilize the structure, and that solvent annealing pathways are important in the self-assembly of complex macrocycle systems.

ASSOCIATED CONTENT

Supporting Information

The Supporting Information is available free of charge at https://pubs.acs.org/doi/10.1021/acs.jpcc.9b11867.

Additional information about STM procedures, STM image analysis, methods for force field development, MD simulations, supplemental STM and MD results (PDF)

AUTHOR INFORMATION

Corresponding Author

Steven L. Tait − *Molecular Materials Design Laboratory, Department of Chemistry, Indiana University, Bloomington, Indiana 47405, United States;* orcid.org/0000-0001-8251-5232; Email: tait@indiana.edu

Authors

Henry D. Castillo − *Molecular Materials Design Laboratory, Department of Chemistry, Indiana University, Bloomington, Indiana 47405, United States*

Jing Yang − *Molecular Materials Design Laboratory, Department of Chemistry, Indiana University, Bloomington, Indiana 47405, United States*

Sibali Debnath − *Molecular Materials Design Laboratory, Department of Chemistry, Indiana University, Bloomington, Indiana 47405, United States*

James R. Dobscha − *Molecular Materials Design Laboratory, Department of Chemistry, Indiana University, Bloomington, Indiana 47405, United States*

Colleen Q. Trainor − *Molecular Materials Design Laboratory, Department of Chemistry, Indiana University, Bloomington, Indiana 47405, United States*

Riley D. Mortensen − *Molecular Materials Design Laboratory, Department of Chemistry, Indiana University, Bloomington, Indiana 47405, United States*

Krishnan Raghavachari − *Molecular Materials Design Laboratory, Department of Chemistry, Indiana University, Bloomington, Indiana 47405, United States;* orcid.org/0000-0003-3275-1426

Amar H. Flood − *Molecular Materials Design Laboratory, Department of Chemistry, Indiana University, Bloomington, Indiana 47405, United States;* orcid.org/0000-0002-2764-9155

Peter J. Ortoleva − *Molecular Materials Design Laboratory, Department of Chemistry, Indiana University, Bloomington,*

https://dx.doi.org/10.1021/acs.jpcc.9b11867
J. Phys. Chem. C 2020, 124, 6689−6699

Indiana 47405, United States; orcid.org/0000-0001-9070-1617

Complete contact information is available at: https://pubs.acs.org/10.1021/acs.jpcc.9b11867

Author Contributions

H.D.C and J.Y. contributed equally to this work.

Notes

The authors declare no competing financial interest.

■ ACKNOWLEDGMENTS

This work was supported by the National Science Foundation, Designing Materials to Revolutionize and Engineer the Future (NSF-DMR-1533988). We acknowledge support for this work from Indiana University's Office of the Vice President for Research, College of Arts & Sciences, and Department of Chemistry. MD calculations were conducted on Indiana University's Big Red II supercomputer supported in part by Lilly Endowment, Inc., through support of Indiana University Pervasive Technology Institute, and in part by the Indiana METACyt Initiative. C.Q.T. was supported by the IU NSF REU program (CHE-1460720).

■ REFERENCES

(1) Rabe, J. P.; Buchholz, S. Commensurability and Mobility in Two-Dimensional Molecular Patterns on Graphite. *Science* **1991**, *253*, 424−427.

(2) Goronzy, D. P.; Ebrahimi, M.; Rosei, F.; Arramel; Fang, Y.; De Feyter, S.; Tait, S. L.; Wang, C.; Beton, P. H.; Wee, A. T. S.; Weiss, P. S.; Perepichka, D. F. Supramolecular Assemblies on Surfaces: Nanopatterning, Functionality, and Reactivity. *ACS Nano* **2018**, *12*, 7445−7481.

(3) Ahn, S.; Matzger, A. J. Six Different Assemblies from One Building Block: Two-Dimensional Crystallization of an Amide Amphiphile. *J. Am. Chem. Soc.* **2010**, *132*, 11364−11371.

(4) Lei, S.; Tahara, K.; De Schryver, F. C.; Van der Auweraer, M.; Tobe, Y.; De Feyter, S. One Building Block, Two Different Supramolecular Surface-Confined Patterns: Concentration in Control at the Solid−Liquid Interface. *Angew. Chem., Int. Ed.* **2008**, *47*, 2964−2968.

(5) Shen, X.; Wei, X.; Tan, P.; Yu, Y.; Yang, B.; Gong, Z.; Zhang, H.; Lin, H.; Li, Y.; Li, Q.; Xie, Y.; Chi, L. Concentration-Controlled Reversible Phase Transitions in Self-Assembled Monolayers on HOPG Surfaces. *Small* **2015**, *11*, 2284−2290.

(6) Hirsch, B. E.; McDonald, K. P.; Qiao, B.; Flood, A. H.; Tait, S. L. Selective Anion-Induced Crystal Switching and Binding in Surface Monolayers Modulated by Electric Fields from Scanning Probes. *ACS Nano* **2014**, *8*, 10858−10869.

(7) Hirsch, B. E.; McDonald, K. P.; Flood, A. H.; Tait, S. L. Living on the Edge: Tuning Supramolecular Interactions to Design Two-Dimensional Organic Crystals Near the Boundary of Two Stable Structural Phases. *J. Chem. Phys.* **2015**, *142*, 101914.

(8) Kim, S.; Castillo, H. D.; Lee, M.; Mortensen, R. D.; Tait, S. L.; Lee, D. From Foldable Open Chains to Shape-Persistent Macrocycles: Synthesis, Impact on 2D Ordering, and Stimulated Self-Assembly. *J. Am. Chem. Soc.* **2018**, *140*, 4726−4735.

(9) Dobscha, J. R.; Castillo, H. D.; Li, Y.; Fadler, R. E.; Taylor, R. D.; Brown, A. A.; Trainor, Q. C.; Tait, S. L.; Flood, A. H. Sequence-Defined Macrocycles for Understanding and Controlling the Build-Up of Hierarchical Order in Self-Assembled 2D Arrays. *J. Am. Chem. Soc.* **2019**, *141*, 17588−17600.

(10) Kampschulte, L.; Lackinger, M.; Maier, A.-K.; Kishore, R. S.; Griessl, S.; Schmittel, M.; Heckl, W. M. Solvent Induced Polymorphism in Supramolecular 1, 3, 5-Benzenetribenzoic Acid Monolayers. *J. Phys. Chem. B* **2006**, *110*, 10829−10836.

(11) Blunt, M. O.; Adisoejoso, J.; Tahara, K.; Katayama, K.; Van der Auweraer, M.; Tobe, Y.; De Feyter, S. Temperature-Induced Structural Phase Transitions in a Two-Dimensional Self-Assembled Network. *J. Am. Chem. Soc.* **2013**, *135*, 12068−12075.

(12) Cui, D.; Ebrahimi, M.; Rosei, F.; Macleod, J. M. Control of Fullerene Crystallization from 2D to 3D through Combined Solvent and Template Effects. *J. Am. Chem. Soc.* **2017**, *139*, 16732−16740.

(13) Ha, N. T. N.; Gopakumar, T. G.; Gutzler, R.; Lackinger, M.; Tang, H.; Hietschold, M. Influence of Solvophobic Effects on Self-Assembly of Trimesic Acid at the Liquid−Solid Interface. *J. Phys. Chem. C* **2010**, *114*, 3531−3536.

(14) Lackinger, M.; Griessl, S.; Heckl, W. M.; Hietschold, M.; Flynn, G. W. Self-Assembly of Trimesic Acid at the Liquid-Solid Interface−A Study of Solvent-Induced Polymorphism. *Langmuir* **2005**, *21*, 4984−4988.

(15) Mamdouh, W.; Uji-i, H.; Ladislaw, J. S.; Dulcey, A. E.; Percec, V.; De Schryver, F. C.; De Feyter, S. Solvent Controlled Self-Assembly at the Liquid-Solid Interface Revealed by STM. *J. Am. Chem. Soc.* **2006**, *128*, 317−325.

(16) Saha, P.; Gurunarayanan, V.; Korolkov, V. V.; Vasudev, P. G.; Ramapanicker, R.; Beton, P. H.; Gopakumar, T. G. Selection of Adlayer Patterns of 1,3-Dithia Derivatives of Ferrocene by the Nature of the Solvent. *J. Phys. Chem. C* **2018**, *122*, 19067−19074.

(17) Tahara, K.; Furukawa, S.; Uji-i, H.; Uchino, T.; Ichikawa, T.; Zhang, J.; Mamdouh, W.; Sonoda, M.; De Schryver, F. C.; De Feyter, S.; Tobe, Y. Two-Dimensional Porous Molecular Networks of Dehydrobenzo[12]annulene Derivatives via Alkyl Chain Interdigitation. *J. Am. Chem. Soc.* **2006**, *128*, 16613−16625.

(18) Hipps, K. W.; Mazur, U. Kinetic and Thermodynamic Control in Porphyrin and Phthalocyanine Self-Assembled Monolayers. *Langmuir* **2018**, *34*, 3−17.

(19) Mazur, U.; Hipps, K. W. Kinetic and Thermodynamic Processes of Organic Species at the Solution−Solid Interface: The View through an STM. *Chem. Commun.* **2015**, *51*, 4737−4749.

(20) Song, W.; Martsinovich, N.; Heckl, W. M.; Lackinger, M. Thermodynamics of 4,4′-Stilbenedicarboxylic Acid Monolayer Self-Assembly at the Nonanoic Acid−Graphite Interface. *Phys. Chem. Chem. Phys.* **2014**, *16*, 13239−13247.

(21) Song, W.; Martsinovich, N.; Heckl, W. M.; Lackinger, M. Thermodynamics of Halogen Bonded Monolayer Self-Assembly at the Liquid−Solid Interface. *Chem. Commun.* **2014**, *50*, 13465−13468.

(22) Song, W.; Martsinovich, N.; Heckl, W. M.; Lackinger, M. Born−Haber Cycle for Monolayer Self-Assembly at the Liquid−Solid Interface: Assessing the Enthalpic Driving Force. *J. Am. Chem. Soc.* **2013**, *135*, 14854−14862.

(23) Simão, C.; Khunsin, W.; Kehagias, N.; Salaun, M.; Zelsmann, M.; Morris, M. A.; Sotomayor Torres, C. M. Order Quantification of Hexagonal Periodic Arrays Fabricated by *in situ* Solvent-Assisted Nanoimprint Lithography of Block Copolymers. *Nanotechnology* **2014**, *25*, 175703.

(24) Sinturel, C.; Vayer, M.; Morris, M.; Hillmyer, M. A. Solvent Vapor Annealing of Block Polymer Thin Films. *Macromolecules* **2013**, *46*, 5399−5415.

(25) Weller, D. W.; Galuska, L.; Wang, W.; Ehlenburg, D.; Hong, K.; Gu, X. Roll-to-Roll Scalable Production of Ordered Microdomains through Nonvolatile Additive Solvent Annealing of Block Copolymers. *Macromolecules* **2019**, *52*, 5026−5032.

(26) Zomerman, D.; Kong, J.; McAfee, S. M.; Welch, G. C.; Kelly, T. L. Control and Characterization of Organic Solar Cell Morphology Through Variable-Pressure Solvent Vapor Annealing. *ACS Appl. Energy Mater.* **2018**, *1*, 5663−5674.

(27) Huang, J.-H.; Li, K.-C.; Chien, F.-C.; Hsiao, Y.-S.; Kekuda, D.; Chen, P.; Lin, H.-C.; Ho, K.-C.; Chu, C.-W. Correlation between Exciton Lifetime Distribution and Morphology of Bulk Heterojunction Films after Solvent Annealing. *J. Phys. Chem. C* **2010**, *114*, 9062−9069.

(28) Kim, G. W.; Kwon, E. H.; Kim, M.; Park, Y. D. Uniform and Reliable Dip-Coated Conjugated Polymers for Organic Transistors as

Obtained by Solvent Vapor Annealing. *J. Phys. Chem. C* **2019**, *123*, 23255−23263.
(29) Na, J. Y.; Kim, M.; Park, Y. D. Solution Processing with a Good Solvent Additive for Highly Reliable Organic Thin-Film Transistors. *J. Phys. Chem. C* **2017**, *121*, 13930−13937.
(30) Sharenko, A.; Gehrig, D.; Laquai, F.; Nguyen, T.-Q. The Effect of Solvent Additive on the Charge Generation and Photovoltaic Performance of a Solution-Processed Small Molecule: Perylene Diimide Bulk Heterojunction Solar Cell. *Chem. Mater.* **2014**, *26*, 4109−4118.
(31) Son, J. G.; Chang, J.-B.; Berggren, K. K.; Ross, C. A. Assembly of Sub-10-nm Block Copolymer Patterns with Mixed Morphology and Period Using Electron Irradiation and Solvent Annealing. *Nano Lett.* **2011**, *11*, 5079−5084.
(32) van Franeker, J. J.; Turbiez, M.; Li, W.; Wienk, M. M.; Janssen, R. A. J. A Real-Time Study of the Benefits of Co-Solvents in Polymer Solar Cell Processing. *Nat. Commun.* **2015**, *6*, 6229.
(33) Amabilino, D.; Bâldea, I.; Batteas, J.; Besenius, P.; Beton, P.; Buck, M.; Chi, L.; Costantini, G.; Davies, P.; De Feyter, S.; Diaz Fernandez, Y.; Dwivedi, D.; Ernst, K.-H.; Flood, A.; Hirsch, B.; Humblot, V.; Jones, R.; Kühnle, A.; Lackinger, M.; Lin, N.; Linderoth, T. R.; Pradier, C.-M.; Rahman, T.; Raval, R.; Robinson, N.; Sacchi, M.; Schwaminger, S.; Tait, S. L.; Woodruff, P.; Zuilhof, H. Supramolecular Effects in Self-Assembled Monolayers: General Discussion. *Faraday Discuss.* **2017**, *204*, 123−158.
(34) Raval, R. Molecular Assembly at Surfaces: Progress and Challenges. *Faraday Discuss.* **2017**, *204*, 9−33.
(35) Haq, S.; Liu, N.; Humblot, V.; Jansen, A. P. J.; Raval, R. Drastic Symmetry Breaking in Supramolecular Organization of Enantiomerically Unbalanced Monolayers at Surfaces. *Nat. Chem.* **2009**, *1*, 409−414.
(36) Gong, J.-R.; Lei, S.-B.; Wan, L.-J.; Deng, G.-J.; Fan, Q.-H.; Bai, C.-L. Structure and Dynamic Process of Two-Dimensional Monodendron Assembly. *Chem. Mater.* **2003**, *15*, 3098−3104.
(37) Bellec, A.; Arrigoni, C.; Schull, G.; Douillard, L.; Fiorini-Debuisschert, C.; Mathevet, F.; Kreher, D.; Attias, A.-J.; Charra, F. Solution-Growth Kinetics and Thermodynamics of Nanoporous Self-Assembled Molecular Monolayers. *J. Chem. Phys.* **2011**, *134*, 124702.
(38) Blunt, M. O.; Russell, J. C.; Giménez-López, M. d. C.; Garrahan, J. P.; Lin, X.; Schröder, M.; Champness, N. R.; Beton, P. H. Random Tiling and Topological Defects in a Two-Dimensional Molecular Network. *Science* **2008**, *322*, 1077−1081.
(39) Cometto, F.; Frank, K.; Stel, B.; Arisnabarreta, N.; Kern, K.; Lingenfelder, M. The STM Bias Voltage-Dependent Polymorphism of a Binary Supramolecular Network. *Chem. Commun.* **2017**, *53*, 11430−11432.
(40) Ahn, S.; Matzger, A. J. Additive Perturbed Molecular Assembly in Two-Dimensional Crystals: Differentiating Kinetic and Thermodynamic Pathways. *J. Am. Chem. Soc.* **2012**, *134*, 3208−3214.
(41) Babu, M. M.; Kriwacki, R. W.; Pappu, R. V. Versatility from Protein Disorder. *Science* **2012**, *337*, 1460−1461.
(42) Whitford, P. C.; Sanbonmatsu, K. Y.; Onuchic, J. N. Biomolecular Dynamics: Order-Disorder Transitions and Energy Landscapes. *Rep. Prog. Phys.* **2012**, *75*, 076601.
(43) Mendoza-Espinosa, P.; García-González, V.; Moreno, A.; Castillo, R.; Mas-Oliva, J. Disorder-to-Order Conformational Transitions in Protein Structure and Its Relationship to Disease. *Mol. Cell. Biochem.* **2009**, *330*, 105−120.
(44) Moritsugu, K.; Terada, T.; Kidera, A. Disorder-to-Order Transition of an Intrinsically Disordered Region of Sortase Revealed by Multiscale Enhanced Sampling. *J. Am. Chem. Soc.* **2012**, *134*, 7094−7101.
(45) Bates, F. S.; Fredrickson, G. H. Block Copolymer Thermodynamics: Theory and Experiment. *Annu. Rev. Phys. Chem.* **1990**, *41*, 525−557.
(46) Köhler, A.; Hoffmann, S. T.; Bässler, H. An Order−Disorder Transition in the Conjugated Polymer MEH-PPV. *J. Am. Chem. Soc.* **2012**, *134*, 11594−11601.
(47) Cortese, J.; Soulié-Ziakovic, C.; Cloitre, M.; Tencé-Girault, S.; Leibler, L. Order−Disorder Transition in Supramolecular Polymers. *J. Am. Chem. Soc.* **2011**, *133*, 19672−19675.
(48) Guice, K. B.; Loo, Y.-L. Reversible Phase Transformations in Concentrated Aqueous Block Copolymer Solutions of Poly(methyl acrylate)-b-poly(hydroxyethyl methacrylate-co-dimethylaminoethyl methacrylate). *Macromolecules* **2007**, *40*, 9053−9058.
(49) Hailey, A. K.; Petty, A. J., II; Washbourne, J.; Thorley, K. J.; Parkin, S. R.; Anthony, J. E.; Loo, Y.-L. Understanding the Crystal Packing and Organic Thin-Film Transistor Performance in Isomeric Guest−Host Systems. *Adv. Mater.* **2017**, *29*, 1700048.
(50) Castillo, H. D.; Espinosa-Duran, J. M.; Dobscha, J. R.; Ashley, D. C.; Debnath, S.; Hirsch, B. E.; Schrecke, S. R.; Baik, M.-H.; Ortoleva, P. J.; Raghavachari, K.; Flood, A. H.; Tait, S. L.; et al. Amphiphile Self-Assembly Dynamics at the Solution-Solid Interface Reveal Asymmetry in Head/Tail Desorption. *Chem. Commun.* **2018**, *54*, 10076−10079.
(51) Xiong, Y.; Cao, T.; Chen, Q.; Li, Z.; Yang, Y.; Xu, S.; Yuan, S.; Sjöblom, J.; Xu, Z. Adsorption of a Polyaromatic Compound on Silica Surfaces from Organic Solvents Studied by Molecular Dynamics Simulation and AFM Imaging. *J. Phys. Chem. C* **2017**, *121*, 5020−5028.
(52) Liu, Y.; Singharoy, A.; Mayne, C. G.; Sengupta, A.; Raghavachari, K.; Schulten, K.; Flood, A. H. Flexibility Coexists with Shape-Persistence in Cyanostar Macrocycles. *J. Am. Chem. Soc.* **2016**, *138*, 4843−4851.
(53) Piskorz, T. K.; de Vries, A. H.; De Feyter, S.; van Esch, J. H. Mechanism of Ostwald Ripening in 2D Physisorbed Assemblies at Molecular Time and Length Scale by Molecular Dynamics Simulations. *J. Phys. Chem. C* **2018**, *122*, 24380−24385.
(54) Minoia, A.; Destoop, I.; Ghijsens, E.; De Feyter, S.; Tahara, K.; Tobe, Y.; Lazzaroni, R. Design of Efficient Sergeant Molecules for Chiral Induction in Nano-Porous Supramolecular Assemblies. *RSC Adv.* **2015**, *5*, 6642−6646.
(55) Palma, C.-A.; Ciesielski, A.; Öner, M. A.; Schaeffer, G.; Lehn, J.-M.; Barth, J. V.; Samorì, P. Two-Dimensional Soft Supramolecular Networks. *Chem. Commun.* **2015**, *51*, 17297−17300.
(56) Debnath, S.; Yang, J.; Ortoleva, P.; Raghavachari, K. Understanding the Origin of 2D Self-Assembly of Tricarbazole Macrocycles: An Integrated Quantum Mechanical/Molecular Dynamics Study. *J. Phys. Chem. C* **2019**, *123*, 17616−17623.
(57) Hadden, J. A.; Perilla, J. R.; Schlicksup, C. J.; Venkatakrishnan, B.; Zlotnick, A.; Schulten, K. All-Atom Molecular Dynamics of the HBV Capsid Reveals Insights into Biological Function and Cryo-EM Resolution Limits. *eLife* **2018**, *7*, 32478.
(58) Cleri, F. Surface Ordering of Molecular Structures by Dispersion Forces. *Phys. Rev. B: Condens. Matter Mater. Phys.* **2009**, *80*, 235406.
(59) Lee, S.; Hirsch, B. E.; Liu, Y.; Dobscha, J. R.; Burke, D. W.; Tait, S. L.; Flood, A. H. Multifunctional Tricarbazolo Triazolophane Macrocycles: One-Pot Preparation, Anion Binding, and Hierarchical Self-Organization of Multilayers. *Chem. - Eur. J.* **2016**, *22*, 560−569.
(60) Dobscha, J. R.; Debnath, S.; Fadler, R. E.; Fatila, E. M.; Pink, M.; Raghavachari, K.; Flood, A. H. Host−Host Interactions Control Self-Assembly and Switching of Triple and Double Decker Stacks of Tricarbazole Macrocycles Co-Assembled with Anti-Electrostatic Bisulfate Dimers. *Chem. - Eur. J.* **2018**, *24*, 9841−9852.
(61) Hess, B.; Kutzner, C.; van der Spoel, D.; Lindahl, E. GROMACS 4: Algorithms for Highly Efficient, Load-Balanced, and Scalable Molecular Simulation. *J. Chem. Theory Comput.* **2008**, *4*, 435−447.
(62) Van Der Spoel, D.; Lindahl, E.; Hess, B.; Groenhof, G.; Mark, A. E.; Berendsen, H. J. C. GROMACS: Fast, Flexible, and Free. *J. Comput. Chem.* **2005**, *26*, 1701−1718.
(63) Humphrey, W.; Dalke, A.; Schulten, K. VMD: Visual Molecular Dynamics. *J. Mol. Graphics* **1996**, *14*, 33−38.
(64) Bussi, G.; Donadio, D.; Parrinello, M. Canonical Sampling through Velocity Rescaling. *J. Chem. Phys.* **2007**, *126*, 014101.

https://dx.doi.org/10.1021/acs.jpcc.9b11867
J. Phys. Chem. C 2020, 124, 6689−6699

(65) Tironi, I. G.; Sperb, R.; Smith, P. E.; van Gunsteren, W. F. A Generalized Reaction Field Method for Molecular Dynamics Simulations. *J. Chem. Phys.* **1995**, *102*, 5451−5459.
(66) Dragoe, N.; Bérardan, D. Order Emerging from Disorder. *Science* **2019**, *366*, 573−574.
(67) Coenen, M. J. J.; Cremers, M.; den Boer, D.; van den Bruele, F. J.; Khoury, T.; Sintic, M.; Crossley, M. J.; van Enckevort, W. J. P.; Hendriksen, B. L. M.; Elemans, J. A. A. W.; Speller, S.; et al. Little Exchange at the Liquid/Solid Interface: Defect-Mediated Equilibration of Physisorbed Porphyrin Monolayers. *Chem. Commun.* **2011**, *47*, 9666−9668.
(68) Shen, M.; Luo, Z.; Zhang, S.; Wang, S.; Cao, L.; Geng, Y.; Deng, K.; Zhao, D.; Duan, W.; Zeng, Q. A Size, Shape and Concentration Controlled Self-Assembling Structure with Host−Guest Recognition at the Liquid−Solid Interface Studied by STM. *Nanoscale* **2016**, *8*, 11962−11968.
(69) Gutzler, R.; Sirtl, T.; Dienstmaier, J. F.; Mahata, K.; Heckl, W. M.; Schmittel, M.; Lackinger, M. Reversible Phase Transitions in Self-Assembled Monolayers at the Liquid−Solid Interface: Temperature-Controlled Opening and Closing of Nanopores. *J. Am. Chem. Soc.* **2010**, *132*, 5084−5090.
(70) Saiz-Poseu, J.; Faraudo, J.; Figueras, A.; Alibes, R.; Busqué, F.; Ruiz-Molina, D. Switchable Self-Assembly of a Bioinspired Alkyl Catechol at a Solid/Liquid Interface: Competitive Interfacial, Noncovalent, and Solvent Interactions. *Chem. - Eur. J.* **2012**, *18*, 3056−3063.
(71) Li, Y.; Flood, A. H. Strong, Size-Selective, and Electronically Tunable C−H···Halide Binding with Steric Control over Aggregation from Synthetically Modular, Shape-Persistent [3_4]Triazolophanes. *J. Am. Chem. Soc.* **2008**, *130*, 12111−12122.
(72) Qiao, B.; Hirsch, B. E.; Lee, S.; Pink, M.; Chen, C.-H.; Laursen, B. W.; Flood, A. H. Ion-Pair Oligomerization of Chromogenic Triangulenium Cations with Cyanostar-Modified Anions that Controls Emission in Hierarchical Materials. *J. Am. Chem. Soc.* **2017**, *139*, 6226−6233.
(73) Copie, G.; Cleri, F.; Makoudi, Y.; Krzeminski, C.; Berthe, M.; Cherioux, F.; Palmino, F.; Grandidier, B. Surface-Induced Optimal Packing of Two-Dimensional Molecular Networks. *Phys. Rev. Lett.* **2015**, *114*, 066101.
(74) Copie, G.; Makoudi, Y.; Krzeminski, C.; Chérioux, F.; Palmino, F.; Lamare, S.; Grandidier, B.; Cleri, F. Atomic Scale Modeling of Two-Dimensional Molecular Self-Assembly on a Passivated Si Surface. *J. Phys. Chem. C* **2014**, *118*, 12817−12825.
(75) Nelyubina, Y. V.; Glukhov, I. V.; Antipin, M. Y.; Lyssenko, K. A. "Higher Density Does Not Mean Higher Stability" Mystery of Paracetamol Finally Unraveled. *Chem. Commun.* **2010**, *46*, 3469−3471.
(76) Cyganik, P.; Buck, M. Polymorphism in Biphenyl-Based Self-Assembled Monolayers of Thiols. *J. Am. Chem. Soc.* **2004**, *126*, 5960−5961.
(77) Cyganik, P.; Buck, M.; Strunskus, T.; Shaporenko, A.; Wilton-Ely, J. D. E. T.; Zharnikov, M.; Wöll, C. Competition as a Design Concept: Polymorphism in Self-Assembled Monolayers of Biphenyl-Based Thiols. *J. Am. Chem. Soc.* **2006**, *128*, 13868−13878.

https://dx.doi.org/10.1021/acs.jpcc.9b11867
J. Phys. Chem. C 2020, 124, 6689−6699